International Journal Software Engineering and Computer Science (IJSECS)
6 (3), 2026, 908-915
Published Online December 2026 in IJSECS (http://www.journal.lembagakita.com/index.php/ijsecs)
P-ISSN: 2776-4869, E-ISSN: 2776-3242. DOI: https://doi.org/10.35870/ijsecs.v6i3.7589.

RESEARCH ARTICLE Open Access

# A Probability-Based Reliability Model for Evaluating Ro-Ro Ferry Sailing-Speed Compliance on an Indonesian Short-Sea Route Using AIS Data

**Hardiyanto [1*], Andri Nofiar. Am [2], Teguh Widodo [3], Supria [4], Depandi Enda [5], Zulyani [6]**

[1*] Department of Maritime, Politeknik Negeri Bengkalis, Bengkalis Regency, Riau Province, Indonesia.
[2] Department of Digital Business, Politeknik Negeri Bengkalis, Bengkalis Regency, Riau Province, Indonesia.
[3] Department of Business Administration, Politeknik Negeri Bengkalis, Bengkalis Regency, Riau Province, Indonesia.
[4] Department of Informatics Engineering, Politeknik Negeri Bengkalis, Bengkalis Regency, Riau Province, Indonesia.
[5] Department of Software Engineering, Politeknik Negeri Bengkalis, Bengkalis Regency, Riau Province, Indonesia.
[6] Department of Shipping Management, Politeknik Negeri Bengkalis, Bengkalis Regency, Riau Province, Indonesia.

**Article History:**

Received: June 16, 2026.
Revised: June 18, 2026.
Accepted: June 20, 2026.
Available online: September 20, 2026.
Published: December 1, 2026.

***Corresponding Author:**
hardiyanto@polbeng.ac.id

**Abstract**: Automatic Identification System (AIS) data provide continuous operational records that can be transformed into computational indicators for evaluating maritime service performance. This study aims to develop an AIS-based probabilistic model for assessing Ro-Ro ferry service-speed reliability through sailing-speed compliance. Speed over Ground (SOG) observations were used to determine whether vessels operated within a predefined reliable speed range during sailing. The reliable speed range was defined as 7–9 knots based on the performance indicator required by the local transportation authority responsible for route licensing, while sailing observations were identified using a 3–15 knot SOG filter. From 32,358 raw AIS messages collected between 1 January and 31 March 2026, 11,166 sailing observations were retained. Observation-based reliability was 35.63%, while duration-based reliability was 36.63%, indicating that 324.76 of 886.64 estimated sailing hours were spent within the reliable speed range. Vessel-level analysis showed substantial variation, with two vessels recording duration-based reliability above 50% and two others below 10%. The Weibull distribution provided the best parametric fit, with an Akaike Information Criterion (AIC) of 44,051.48, the lowest among the fitted candidate distributions. The cumulative distribution function indicated a 35.88% probability of operating within the 7–9 knot range. Monte Carlo bootstrap resampling with 10,000 iterations produced 95% confidence intervals of 34.75–36.53% and 35.38–37.88% for observation-based and duration-based reliability, respectively. These findings indicate that AIS data can support a reproducible screening approach for evaluating aggregate and vessel-level ferry service-speed reliability.

**Keywords**: Automatic Identification System (AIS); service-speed reliability; probability distribution; Weibull distribution; Monte Carlo simulation; Ro-Ro ferry.

## 1. Introduction

Ro-Ro ferry services are essential components of short-sea transport systems because they support passenger mobility, vehicle transfer, and regional logistics connectivity. In short-sea corridors, service performance can be affected by vessel availability, terminal operations, sailing regularity, and the ability of vessels to maintain an expected operating condition during a crossing. Among these operational variables, Speed over Ground (SOG) is one of the most directly observable indicators available from Automatic Identification System (AIS) data. Although SOG does not represent the overall quality of ferry service, it provides a measurable basis for evaluating whether a vessel operates within a predefined service-speed envelope while sailing.

AIS data have been widely used in maritime analytics because they provide repeated records of vessel identity, timestamp, position, course, and speed. Recent studies have applied AIS data to maritime anomaly detection, trajectory prediction, operational monitoring, and port-efficiency measurement. Nguyen *et al.* (2020) demonstrated the operational relevance of AIS-based detection of abnormal vessel behaviour, while Singh and Heymann (2020) used AIS-derived position, speed, course, and timing features for maritime anomaly detection. Capobianco *et al.* (2021) showed that historical AIS observations can support vessel trajectory prediction using deep learning, while Martinčič *et al.* (2020) emphasized the role of validated AIS data in constructing vessel and port-efficiency metrics. Li *et al.* (2023a) also demonstrated the use of AIS data for ship trajectory prediction using machine learning and deep learning methods. Together, these studies demonstrate that AIS data can support not only navigation-related analysis but also the assessment of vessel and maritime transport performance.

Despite these developments, most AIS-based maritime studies focus on trajectory prediction, anomaly detection, traffic monitoring, and port-efficiency indicators rather than threshold-based service reliability. In ferry operations, reliability is commonly associated with schedule adherence, travel-time variability, headway regularity, and terminal performance. Transportation reliability research also indicates that performance consistency can be evaluated using probability-based and distribution-based measures when an acceptable operating range or threshold is defined. Zang *et al.* (2022) reviewed methodological developments in travel-time reliability and emphasized the use of distributional and probability-based approaches for evaluating transport-system performance under variable conditions. However, limited attention has been given to AIS-derived reliability measures that assess ferry service-speed compliance using both observation-based and duration-based indicators.

This study addresses this gap by developing a simplified observation-level probabilistic model for evaluating Ro-Ro ferry service-speed reliability from AIS data. The model defines reliable operation as compliance with a sailing-speed interval of 7–9 knots and applies a 3–15 knot filter to identify sailing observations. The 7–9 knot interval was not selected as an arbitrary statistical threshold; it was defined based on the performance indicator required by the local transportation authority responsible for route licensing. Therefore, the threshold represents an operational service-speed envelope used to assess whether observed Ro-Ro ferry operations comply with the expected sailing-speed condition on the permitted route. Reliability is measured using two complementary indicators: observation-based reliability, which estimates the proportion of AIS observations within the reliable-speed range, and duration-based reliability, which estimates the proportion of valid sailing time spent within that range. The second measure accounts for differences in the spacing of AIS observations and provides a time-based complement to the observation-count measure.

In contrast to AIS studies that mainly use SOG as an input feature for trajectory prediction, anomaly detection, or traffic monitoring, this study treats SOG as an operational compliance variable. The analytical focus is directed toward whether a vessel operates within the expected service-speed envelope while sailing, rather than toward trajectory characteristics alone. This approach links AIS-based maritime analytics with probability-based assessment of service-speed compliance. The main contribution of this study is the formulation of ferry service-speed compliance as a reproducible AIS-derived probabilistic indicator rather than as a conventional trajectory-prediction, anomaly-detection, or schedule-adherence problem. The proposed approach combines speed filtering, binary service-compliance classification, duration-based reliability estimation, reliable-segment analysis, parametric distribution fitting, CDF-based probability estimation, and bootstrap-based uncertainty assessment within a screening-level framework. In this context, the term "first-stage diagnostic tool" refers to an AIS-exclusive screening method for identifying aggregate, temporal, and vessel-specific speed-compliance patterns before more detailed berth-to-berth service-leg reconstruction is undertaken. The method is not intended to provide a causal diagnosis of service delays or operational failures, but to identify patterns that warrant further operational investigation.

## 2. Related Work

### 2.1 AIS-Based Maritime Data Analytics

Automatic Identification System (AIS) data have become an important source for maritime data analytics because they provide spatio-temporal records of vessel identity, position, course, and speed. Recent studies have used AIS data for trajectory prediction, anomaly detection, route extraction, maritime monitoring, and operational decision support. Yang *et al.* (2024) reviewed machine-learning applications using AIS data and discussed the use of large-scale spatio-temporal vessel patterns for maritime decision-making (Liang *et al.*, 2024; Yang *et al.*, 2019). These studies indicate that AIS records can be processed beyond their original navigational purpose to support the analysis of vessel operations. Several studies have focused on trajectory prediction and movement modelling. An AIS-based Bi-LSTM trajectory prediction model showed that denoising, trajectory separation, and standardization can improve prediction accuracy in maritime traffic management (Yang *et al.*, 2022). A systematic review of machine-learning and deep-learning methods for ship trajectory prediction found that AIS-based prediction is mainly directed toward navigation safety, collision prevention, and traffic management (Li *et al.*, 2023b). Historical AIS data have also been used for maritime route extraction by transforming vessel trajectories into semantic trip objects and directed traffic graphs (Yan *et al.*, 2020). Although these studies demonstrate the suitability of AIS data for identifying vessel movement patterns, their primary focus remains on trajectory modelling, route extraction, and navigational decision support. AIS data have also been widely applied to anomaly detection. Wolsing *et al.* (2022) reviewed 44 studies on maritime AIS anomaly detection and reported that AIS-based anomalies are commonly examined in relation to safety, security, collision risk, and abnormal vessel behaviour. This deviation-based approach is conceptually relevant to the present study because both approaches compare observed vessel behaviour with an expected condition. However, rather than defining deviation in terms of safety or security anomalies, the present study evaluates compliance with a predefined sailing-speed requirement for Ro-Ro ferry operations.

### 2.2 Reliability and Probabilistic Assessment in Maritime Transportation

Reliability-oriented approaches have been applied in maritime and waterway transportation to evaluate system performance, resilience, and operational risk. Wang and Yuen (2022) developed a resilience assessment model for waterway transportation systems by combining system performance with recovery cost, using AIS data as an input to a discrete-event simulation. Their study demonstrates that AIS-derived operational information can support performance assessment when vessel delays and system recovery are considered. This perspective is relevant to the present study because it links vessel movement data to quantitative measures of transportation-system performance. Probabilistic approaches provide another means of representing uncertainty in maritime operations. Xin *et al.* (2021) proposed a probabilistic conflict-detection approach for multi-ship collision risk under spatio-temporal movement uncertainty and applied Monte Carlo simulation for risk estimation. Vukša *et al.* (2022) similarly combined Monte Carlo simulation with AIS-based traffic and route information to estimate ship collision probability. Other reliability studies have also applied Monte Carlo methods to quantify uncertainty in operational systems (Arekar *et al.*, 2021; Labeau & Zio, 2002). These studies indicate that probability-based methods can effectively represent variability in observed or simulated operational conditions rather than relying solely on deterministic performance measures.

In a threshold-based assessment, reliability can be defined by specifying an acceptable operational condition and estimating the proportion or probability of observations that satisfy that condition. In the present study, the acceptable condition is defined by compliance with a prescribed sailing-speed range. The distinction between compliance and reliability is essential: compliance refers to whether an individual observation or time interval satisfies the prescribed speed condition, whereas reliability refers to the aggregate proportion of observations or operating time that satisfies this condition. This formulation allows AIS-derived vessel speed to be converted into a measurable operational indicator while maintaining a clear distinction between an individual compliant state and an aggregate reliability measure.

Parametric probability distributions can further characterize the variability of continuous operational measurements. Rather than assuming a particular distribution in advance, distribution fitting identifies whether a parametric model provides an adequate representation of the observed sailing-speed data. The selected distribution can then estimate probabilities associated with the predefined operating range, providing a complementary perspective to direct observation-based and duration-based reliability measures. In addition, bootstrap methods evaluate uncertainty in empirical reliability estimates. By repeatedly resampling the available observations, bootstrap analysis provides an empirical assessment of the stability of an estimated reliability value without requiring the indicator to follow a predetermined theoretical distribution. In AIS-based ferry analysis, this approach complements probability-based modelling by indicating how sensitive the estimated reliability is to sample variability. Although these studies provide robust methodological foundations, their applications primarily concern collision risk, resilience, route prediction, or safety-related operational conditions. Less attention has been given to defining ferry service reliability specifically through compliance with a prescribed sailing-speed range derived from AIS observations. The present study addresses this opportunity by extending probability-based operational assessment toward Ro-Ro ferry service-speed compliance, combining observation-based and duration-based indicators with distributional analysis and bootstrap-based uncertainty assessment.

### 2.3 Position of the Present Study

The present study differs from previous AIS-based maritime analytics in three fundamental aspects. Primarily, it treats AIS-derived Speed over Ground (SOG) as an operational compliance variable rather than as a predictive feature for trajectory estimation or anomaly detection. Furthermore, it formulates Ro-Ro ferry sailing-speed compliance as a service-speed reliability measure by classifying AIS observations against a configured 7–9 knot operating range. Additionally, it complements observation-based reliability with duration-based reliability and reliable-speed segment analysis, thereby mitigating analytical dependence on raw AIS message frequency. This positioning is critical because AIS observations are frequently recorded at irregular temporal intervals. Combining observation-based reliability with duration-based reliability and continuous sailing-speed distributions directly addresses unequal reporting frequencies. Parametric distribution fitting, CDF-based probability estimation, and bootstrap resampling serve as complementary procedures within this screening framework. The model is specifically designed as a first-stage diagnostic assessment of ferry service-speed compliance rather than a substitute for full berth-to-berth service-leg reconstruction.

Table 1. Research Gap Analysis in Relation to Previous Studies

| Study or literature group | Data and method | Main focus | Limitation relative to this study | Position of the present study |
|---|---|---|---|---|
| Yang *et al.* (2024); Yang *et al.* (2019) | AIS-based maritime data mining and machine learning | AIS analytics, maritime data, and operational knowledge extraction | Does not explicitly address ferry service-speed compliance | Uses AIS-derived SOG as an operational compliance variable |
| Wolsing *et al.* (2022) | Review of AIS anomaly-detection studies | Abnormal vessel behaviour and safety/security anomalies | Focuses on anomaly detection rather than service-standard compliance | Applies deviation logic to service-speed compliance |
| Yang *et al.* (2022); Li *et al.* (2023b) | AIS denoising, Bi-LSTM, ML/DL trajectory prediction | Vessel trajectory prediction and navigational decision support | Treats SOG primarily as a trajectory variable | Converts SOG into compliant/non-compliant service states |
| Yan *et al.* (2020) | Historical AIS and route extraction | Maritime route extraction and traffic-pattern construction | Does not explicitly evaluate compliance with a service-speed envelope | Evaluates sailing-speed compliance against an operational threshold |
| Wang and Yuen (2022); Zohoori *et al.* (2023) | AIS-based simulation and resilience assessment | Waterway resilience and system-level performance | Focuses on system resilience rather than vessel-level ferry speed compliance | Provides aggregate and vessel-level speed-compliance diagnostics |
| Xin *et al.* (2021); Vukša *et al.* (2022) | Probabilistic risk assessment and Monte Carlo simulation | Collision risk and maritime safety uncertainty | Applies probability and simulation to safety risk rather than ferry service performance | Applies probabilistic estimation and bootstrap resampling to service-speed reliability |
| Betz *et al.* (2022); Labeau and Zio (2002); Arekar *et al.* (2021) | Reliability theory and Monte Carlo methods | Reliability estimation and uncertainty quantification | Provides methodological foundations but not a ferry-specific AIS compliance model | Combines reliability estimation, candidate distribution fitting, CDF interpretation, and bootstrap uncertainty assessment |
| Present study | AIS-derived SOG, threshold-based compliance, duration weighting, | Ro-Ro ferry service-speed reliability | — | Provides a reproducible AIS-based screening model for aggregate, |

| | | | |
|---|---|---|---|
| | distribution fitting, CDF estimation, and bootstrap | | temporal, and vessel-level speed compliance |

The reviewed studies confirm that AIS data have been extensively leveraged for trajectory prediction, route extraction, anomaly detection, collision-risk evaluation, and waterway resilience assessment. Nevertheless, existing analytical pipelines rarely transform AIS-derived sailing speed into an operational service-standard compliance indicator for ferry operations. The specific gap addressed in this study is therefore both methodological and operational: while current AIS analytics effectively describe vessel movement or detect navigational anomalies, they provide limited insight into how consistently Ro-Ro ferry vessels maintain a mandated service-speed envelope. The present study bridges this gap by integrating observation-based compliance, duration-weighted reliability, parametric distribution fitting, CDF-based probability estimation, and bootstrap resampling into a cohesive screening framework.

## 3. Methodology

### 3.1 Dataset and Preprocessing

The dataset consisted of AIS records from Ro-Ro ferry operations across four vessels. The raw dataset contained 32,358 messages. The *created_at* attribute served as the operational timestamp, while Speed over Ground (SOG) was used as the primary operational variable. Records with missing timestamps or SOG values were removed, along with entries falling outside the initial quality-control threshold of 0–30 knots. A subsequent sailing-state filter retained observations with SOG values between 3 and 15 knots (Deriba & Yang, 2025; Liang *et al.*, 2024). The 0–30 knot boundary was implemented for preliminary data cleaning, whereas the 3–15 knot range was used to extract observations representative of active sailing conditions.

Table 2. Summary of AIS Dataset Preprocessing Stages

| Stage | Number of records | Percentage of raw AIS records (%) |
|---|---|---|
| Raw AIS messages | 32,358 | 100.00 |
| After timestamp and SOG cleaning | 32,352 | 99.98 |
| Sailing observations (3.0–15.0 knots) | 11,166 | 34.51 |
| Reliable observations (7.0–9.0 knots) | 3,978 | 12.29 |
| Non-compliant observations | 7,188 | 22.21 |

The percentages in Table 2 are computed relative to the total raw AIS dataset. In contrast, the observation-based reliability metrics presented in subsequent sections are calculated relative to the retained sailing observations. All analytical routines were executed in Google Colab using Python. The computational environment utilized pandas for data structuring, NumPy for numerical operations, SciPy for statistical analysis and parametric distribution fitting, Matplotlib for data visualization, and openpyxl for tabular data export. Detailed software dependencies and library versions were documented in the notebook environment to ensure full analytical reproducibility.

Figure 1. Analytical Workflow for Processing AIS Data and Estimating Service-Speed Reliability

Figure 1 illustrates the end-to-end analytical workflow, beginning with raw AIS ingestion, data cleaning, and sailing-observation filtering, followed by binary service-speed compliance classification, empirical reliability calculation, duration-based weighting, parametric distribution fitting, CDF probability estimation, and bootstrap resampling for uncertainty assessment. This systematic procedure ensures a transparent and reproducible transformation from raw AIS messages into robust operational reliability indicators.

### 3.2 Speed-Compliance Indicator

The reliable sailing-speed range was defined as 7–9 knots based on the performance indicator required by the local transportation authority responsible for route licensing. This range was used as the operational compliance threshold for evaluating whether each retained AIS-derived sailing observation satisfied the prescribed service-speed condition. The 7–9 knot interval was therefore not treated as an arbitrary statistical threshold but as an operational service-speed envelope for the permitted route. The use of AIS-derived SOG is consistent with previous AIS-based maritime studies in which vessel speed, position, course, and timestamp are used to characterize vessel behaviour and operational patterns (Wolsing *et al.*, 2022; Yang *et al.*, 2024). Each sailing observation was classified using a binary compliance indicator. An observation was assigned a value of 1 when its SOG was within the 7–9 knot range and 0 otherwise. The compliance indicator is defined as:

$$I_i = \begin{cases} 1, & 7 \le SOG_i \le 9 \\ 0, & \text{otherwise} \end{cases} \tag{1}$$

Where $I_i$ denotes the reliability state of the $i$-th sailing observation, and $SOG_i$ denotes the Speed over Ground value of that observation. The observation-based reliability was then calculated as the proportion of sailing observations that satisfied the reliable-speed criterion:

$$R_{obs} = \frac{\sum_{i=1}^{N} I_i}{N} \tag{2}$$

Where Nis the total number of sailing observations after filtering. The corresponding failure probability, representing the proportion of observations outside the reliable speed range, was computed as:

$$P_f = 1 - R_{obs} \tag{3}$$

In this study, non-compliance probability refers to the proportion of retained sailing observations outside the predefined 7–9 knot service-speed envelope. It does not indicate mechanical failure, accident occurrence, or complete service failure. The formulation therefore defines reliability specifically as the proportion of observed sailing states that comply with the prescribed service-speed condition. A sensitivity analysis was conducted to examine whether the reliability estimates were affected by the selected sailing-filter and service-speed parameters. The baseline configuration used a 3–15 knot sailing filter and a 7–9 knot reliable-speed range. Alternative sailing filters with lower boundaries of 2 and 4 knots were also tested, together with wider service-speed ranges of 6.5–9.5, 7–9.5, and 6.5–9 knots. For each scenario, observation-based and duration-based reliability were recalculated using the same computational procedure.

Table 3. Sensitivity Analysis of Sailing Filter and Reliable-Speed Range

| Scenario | Sailing filter knots | Reliable-speed range (knots) | Sailing observations | Reliable observations | Robs*Robs* (%) | Sailing duration (h) | Reliable duration (h) | Rtime*Rtime* (%) |
|---|---|---|---|---|---|---|---|---|
| Baseline | 3–15 | 7–9 | 11,166 | 3,978 | 35.63 | 886.64 | 324.76 | 36.63 |
| S1 | 2–15 | 7–9 | 11,823 | 3,978 | 33.65 | 948.82 | 337.57 | 35.58 |
| S2 | 4–15 | 7–9 | 10,503 | 3,978 | 37.87 | 818.90 | 310.93 | 37.97 |
| S3 | 3–15 | 6.5–9.5 | 1,166 | 5,549 | 49.70 | 886.64 | 458.57 | 51.72 |
| S4 | 3–15 | 7–9.5 | 11,166 | 4,493 | 40.24 | 886.64 | 369.99 | 41.73 |
| S5 | 3–15 | 6.5–9 | 11,166 | 5,034 | 45.08 | 886.64 | 413.34 | 46.62 |

The sensitivity analysis showed that modifying the lower boundary of the sailing filter produced only moderate changes in the reliability estimates. Using a 2–15 knot filter resulted in observation-based and duration-based reliability values of 33.65% and 35.58%, respectively, while the 4–15 knot filter resulted in 37.87% and 37.97%. These values remained relatively close to the baseline duration-based reliability of 36.63%. In contrast, widening the reliable-speed range increased the estimated reliability because a larger proportion of observations satisfied the compliance criterion. For example, extending the range to 6.5–9.5 knots increased duration-based reliability to 51.72%. The baseline 7–9 knot range was retained because it represents the operational service-speed indicator for the observed route, while the alternative configurations were used only for robustness assessment.

### 3.3 Duration-Based Reliability

Reliable sailing duration was estimated after AIS records were sorted separately by vessel identity and timestamp. For each vessel, the time interval between consecutive AIS observations was calculated as:

$$\Delta t_{v,i} = t_{v,i} + 1 - \ t_{v,i} \tag{4}$$

Where v denotes the vessel and I denotes the index of the consecutive observation pair. Only positive intervals not exceeding the maximum allowable AIS gap of 20 minutes were retained as valid sailing intervals. This restriction was applied to reduce the risk of interpreting long AIS transmission gaps as continuous sailing activity. The 20-minute maximum gap was selected based on the operational characteristics of the observed Ro-Ro ferry route. The total crossing time was generally within approximately 40–60 minutes, while the effective sailing-zone interval was approximately 20 minutes. An AIS reporting interval longer than this threshold may bridge unobserved manoeuvring, terminal approach, waiting, or transition periods and therefore may not represent continuous sailing activity. A gap-threshold sensitivity analysis was also conducted. The 15-, 20-, and 30-minute thresholds produced duration-based reliability estimates of 36.86%, 36.63%, and 36.40%, respectively. These results indicate that the estimate was relatively stable around the selected 20-minute threshold. Shorter thresholds reduced the number of valid temporal intervals and could fragment continuous reliable-speed periods, whereas longer thresholds increased the possibility of treating extended periods without AIS observations as continuous sailing activity. The 20-minute threshold was therefore retained as the baseline setting. The total estimated sailing duration was calculated by summing the valid consecutive intervals across all vessels:

$$T_{sailing} = \sum_{v=1}^{v} \quad \sum_{i=1}^{nv-1} \Delta t_{v,i,} \tag{5}$$

Where V denotes the total number of vessels, v is the vessel index, and nv denotes the number of retained observations for vessel v. The reliable sailing duration was calculated by summing the valid intervals associated with observations classified as compliant with the prescribed 7–9 knot range:

$$T_{reliable} = \sum_{v=1}^{v} \quad \sum_{i=1}^{nv-1} c_{v,i,} \Delta t_{v,i,} \tag{6}$$

Where cv,i denotes the binary compliance indicator associated with the observation at the beginning of the i-th valid interval for vessel v. The duration-based reliability was then calculated as:

$$R_{time} = \frac{T_{reliable}}{T_{sailing}} X100\% \tag{7}$$

This metric estimates the proportion of valid sailing time associated with the reliable-speed condition and therefore complements the observation-based reliability measure when AIS observations are not uniformly distributed over time. Reliable-speed segments were also identified to describe the continuity of compliant operation. Consecutive reliable observations from the same vessel were grouped into the same segment when the time interval between observations did not exceed the 20-minute threshold. A new segment was initiated when the vessel identity changed, the observed SOG moved outside the 7–9 knot range, or the time gap exceeded the maximum allowable threshold. The duration of each reliable segment was calculated from its valid consecutive intervals. This segment-level measure provides additional information on whether compliant operation occurred as short isolated periods or as sustained sailing periods.

### 3.4 Probability Distribution Fitting and CDF Analysis

The empirical distribution of sailing speed was first examined using a histogram and kernel density estimation (KDE). These non-parametric representations were used to describe the observed SOG pattern before fitting candidate parametric distributions. Four candidate distributions—Normal, Lognormal, Gamma, and Weibull—were fitted to the retained sailing-speed observations. These distributions were selected as candidate models for representing continuous operational measurements and for enabling probability estimation through their cumulative distribution functions. The best-fitting distribution was determined using the Akaike Information Criterion (AIC), which considers both model fit and the number of estimated parameters. A lower AIC value indicates a more parsimonious model among the candidate distributions. The AIC is calculated as:

$$AIC = 2k - 2\ln(L) \tag{8}$$

Where k denotes the number of estimated parameters and L denotes the maximum likelihood of the fitted model. After the best-fitting distribution was identified, its cumulative distribution function F(x) was used to estimate the probability that the observed sailing speed fell within the prescribed 7–9 knot range:

$$P(7 \leq SOG \leq 9) = F(9) - F(7) \tag{9}$$

This distribution-based probability provides a complementary estimate of service-speed compliance and can be compared directly with the empirical observation-based and duration-based reliability measures.

### 3.5 Bootstrap Uncertainty Assessment

Bootstrap resampling was conducted to assess the sampling uncertainty of the estimated service-speed reliability indicators. The procedure utilized 10,000 bootstrap iterations with a sampling fraction of 1.0, ensuring that each resampled iteration contained the same number of units as the empirical dataset. For observation-based reliability, retained sailing observations were resampled with replacement, and the aggregate reliability metric was recomputed for each iteration. For duration-based reliability, the resampling scheme was designed to preserve the sequential temporal structure necessary for computing consecutive AIS intervals, rather than treating individual observations as independent time intervals. The resulting empirical bootstrap distributions were used to construct 95% confidence intervals, where the lower and upper limits were determined from the 2.5th and 97.5th percentiles, respectively. This non-parametric approach yields an empirical uncertainty range without imposing assumptions regarding the theoretical distribution of the reliability metrics.

## 4. Results and Discussion

### 4.1 Results

A descriptive analysis was conducted to examine the distribution of AIS-derived sailing-speed observations relative to the prescribed 7–9 knot service-speed envelope. A total of 11,166 AIS observations satisfied the baseline sailing filter of 3–15 knots. Of these observations, 3,978 fell within the 7–9 knot reliable-speed range, whereas 7,188 were outside the prescribed service envelope.

Table 4. Descriptive Statistics and Observation-Based Reliability

| Statistic | Value |
|---|---|
| Sailing observations | 11,166 |
| Reliable observations (7–9 knots) | 3,978 |
| Non-compliant observations | 7,188 |
| Mean SOG (knots) | 6.74 |
| Median SOG (knots) | 6.70 |
| SOG standard deviation (knots) | 1.74 |
| Minimum SOG after sailing filter (knots) | 3.00 |
| Maximum SOG after sailing filter (knots) | 12.30 |
| Observation-based reliability (Robs$Robs$, %) | 35.63 |
| Non-compliance probability (Pf$Pf$, %) | 64.37 |

The empirical observation-based reliability was 35.63%, calculated from 3,978 compliant observations out of 11,166 retained sailing records. The complementary non-compliance probability was 64.37%. Across the active sailing dataset, the mean SOG was 6.74 knots and the median SOG was 6.70 knots, both positioned below the 7-knot lower compliance threshold. SOG values ranged from 3.00 to 12.30 knots, with an overall standard deviation of 1.74 knots. Duration-based analysis was subsequently applied to quantify the cumulative sailing time associated with compliant speed conditions. After executing vessel-specific temporal sequencing and applying the 20-minute maximum allowable gap criterion, the total estimated sailing duration across all vessels was 886.64 hours.

Table 5. Duration-Based Reliability and Reliable-Segment Statistics

| Measure | Value |
|---|---|
| Total estimated sailing duration (hours) | 886.64 |
| Total reliable duration, 7–9 knots (hours) | 324.76 |
| Total non-compliant duration (hours) | 561.88 |
| Duration-based reliability (Rtime*Rtime*, %) | 36.63 |
| Non-compliance probability (%) | 63.37 |
| Reliable segments (count) | 1,285 |
| Mean reliable segment duration (minutes) | 15.16 |
| Median reliable segment duration (minutes) | 13.10 |
| Maximum reliable segment duration (minutes) | 40.93 |

As detailed in Table 5, compliant operations accounted for 324.76 hours, yielding a duration-based reliability (Rtime) of 36.63%. Conversely, 561.88 hours (63.37% of the total operating time) failed to satisfy the service-speed requirement. The compliant observations formed 1,285 discrete reliable segments. The mean segment duration was 15.16 minutes, the median was 13.10 minutes, and the maximum recorded segment duration reached 40.93 minutes.

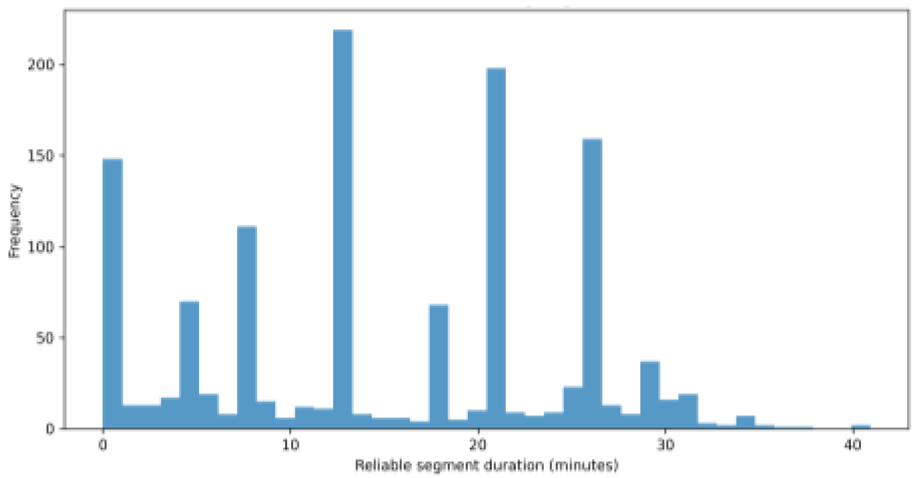


Figure 2. Distribution of Reliable Sailing Segment Duration

Figure 2. illustrates the distribution of reliable-segment durations across the fleet, highlighting the persistence of compliant operational periods. To identify operational heterogeneity within the fleet, both reliability indicators were disaggregated by individual vessel.

Table 6. Vessel-Level Observation and Duration Reliability Metrics

| Vessel | Sailing observations | Reliable observations | Mean SOG (knots) | Robs*Robs* (%) | Rtime*Rtime* (%) | Sailing duration (h) | Reliable duration (h) |
|---|---|---|---|---|---|---|---|
| KMP BN | 3,569 | 2,034 | 7.21 | 56.99 | 61.52 | 279.26 | 171.79 |
| KMP SP | 3,298 | 1,655 | 7.76 | 50.18 | 53.68 | 236.96 | 127.20 |
| KMP SD | 3,491 | 247 | 5.59 | 7.08 | 7.40 | 284.84 | 21.09 |
| KMP MP2 | 808 | 42 | 5.39 | 5.20 | 5.47 | 85.58 | 4.68 |

The vessel-level results in Table 6 demonstrate sharp operational divergence across the fleet. KMP BN achieved the highest performance, recording an observation-based reliability of 56.99% and a duration-based reliability of 61.52% with a mean SOG of 7.21 knots. KMP SP also maintained compliant operations for more than half of its service, exhibiting 50.18% observation reliability, 53.68% duration reliability, and an average speed of 7.76 knots. In stark contrast, KMP SD recorded observation and duration reliabilities of only 7.08% and 7.40%, respectively (mean SOG of 5.59 knots). KMP MP2 recorded the lowest performance, with 5.20% observation reliability, 5.47% duration reliability, and an average SOG of 5.39 knots. To evaluate parametric representations of sailing behavior, four candidate probability distributions were fitted to the sailing-speed observations: Normal, Lognormal, Gamma, and Weibull. Model performance was evaluated using log-likelihood, AIC, and BIC criteria.

Table 7. Parametric Distribution Fitting for Ro-Ro Sailing Speed

| Distribution | Number of parameters (k) | Log-likelihood | AIC | BIC |
|---|---|---|---|---|
| Weibull | 3 | -22,022.74 | 44,051.48 | 44,073.44 |
| Normal | 2 | -22,053.14 | 44,110.28 | 44,124.92 |
| Gamma | 3 | -22,177.56 | 44,361.13 | 44,383.09 |
| Lognormal | 3 | -22,411.42 | 44,828.85 | 44,850.81 |

As summarized in Table 7, the Weibull distribution achieved the best overall fit, yielding the lowest AIC (44,051.48) and BIC (44,073.44). The Normal distribution provided the second-best fit with an AIC of 44,110.28, resulting in a substantial AIC differential (ΔAIC=58.80ΔAIC=58.80) favoring the Weibull model. The fitted Weibull distribution yielded an estimated shape parameter of k=4.3276 and a scale parameter of λ=7.4030.

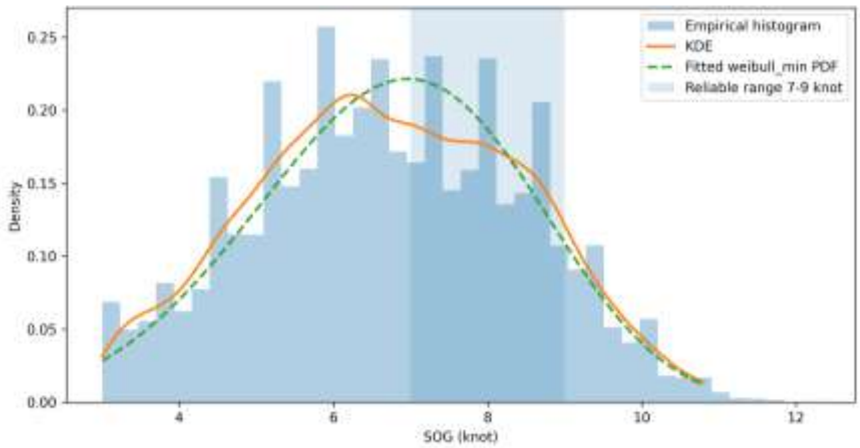


Figure 3. Probability Density Function (PDF) of Sailing Speed Comparing Empirical Histogram, Kernel Density Estimation (KDE), and Fitted Weibull Distribution

Figure 3. compares the empirical speed histogram, non-parametric KDE, and fitted Weibull PDF, confirming that the Weibull model captures the unimodal operational profile of the fleet. The cumulative distribution function of this optimal model was then utilized to evaluate service-speed compliance probability.

Table 8. CDF-Based Interpretation of Sailing-Speed Compliance Under the Fitted Weibull Distribution

| CDF metric | Value |
|---|---|
| Selected distribution | Weibull |
| Cumulative probability below 7 knots, F(7)*F*(7) | 0.5438 |
| Cumulative probability below 9 knots, F(9)*F*(9) | 0.9026 |
| Interval compliance probability, P(7≤SOG≤9)*P*(7≤SOG≤9) | 0.3588 |
| CDF-based service reliability (%) | 35.88 |
| CDF-based non-compliance probability (%) | 64.12 |

Based on the fitted Weibull CDF, the cumulative probability of operating below the lower threshold was F(7)=0.5438, while that below the upper limit was F(9)=0.9026. Evaluating Equation (9) yielded an interval probability of P(7≤SOG≤9)=0.3588, representing a CDF-derived reliability of 35.88% (Table 8). This parametric probability shows remarkable concordance with the empirical observation-based reliability of 35.63%.

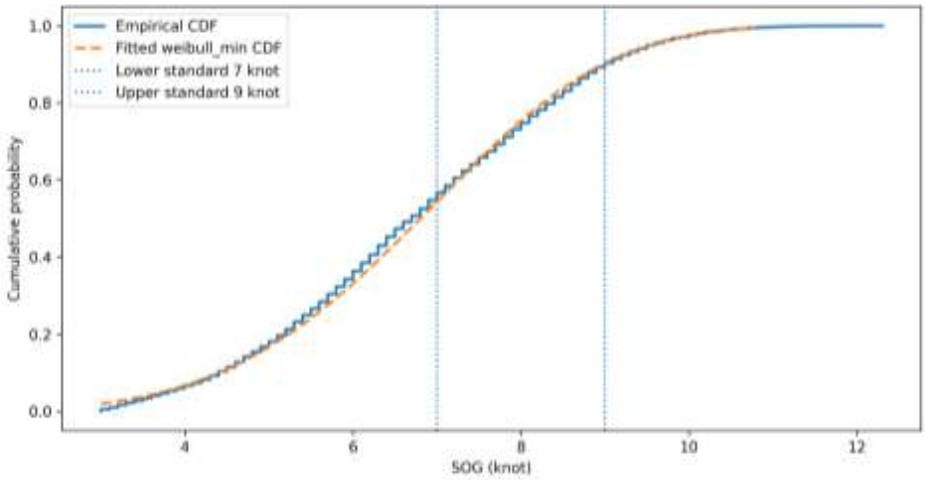


Figure 4.Cumulative Distribution Function (CDF) of Fitted Weibull Sailing Speed with Prescribed 7–9 Knot Service Boundaries

Figure 4. illustrates the cumulative probability progression across operating speeds, highlighting the substantial probability mass (54.38%54.38%) accumulated prior to entering the compliant 7-knot threshold. To assess whether operating compliance remained stable over time, monthly reliability metrics were evaluated across the three-month observation window.

Table 9. Monthly Service-Speed Reliability and Operational Progression

| Month | Sailing observations | Reliable observations | Mean SOG (knots) | Robs*Robs* (%) | Rtime*Rtime* (%) | Reliable duration (h) |
|---|---|---|---|---|---|---|
| 2026-01 | 2,652 | 1,022 | 6.87 | 38.54 | 39.88 | 103.23 |
| 2026-02 | 4,020 | 1,424 | 6.71 | 35.42 | 36.78 | 100.98 |
| 2026-03 | 4,494 | 1,532 | 6.68 | 34.09 | 34.13 | 120.55 |

The monthly evaluation presented in Table 9 demonstrates a downward trend across the monitoring period. Observation-based reliability contracted from 38.54% in January to 35.42% in February and 34.09% in March. Concurrently, duration-based reliability declined from 39.88% to 36.78% and 34.13%. This compliance reduction coincided with an increase in total sailing records (rising from 2,652 in January to 4,494 in March) and a subtle decrease in mean fleet SOG from 6.87 knots to 6.68 knots.

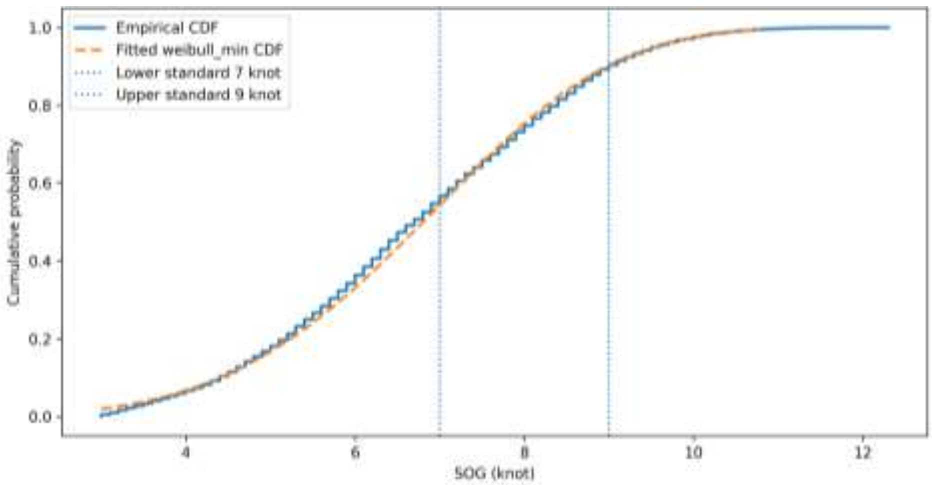


Figure 5. Temporal Trends in Monthly Observation-Based and Duration-Based Service-Speed Reliability

Figure 5. depicts the synchronized contraction of both reliability indicators across the observation timeframe. Finally, to evaluate sampling uncertainty, non-parametric bootstrap resampling was executed across 10,000 iterations for both reliability indicators.

Table 10. Bootstrap Estimation and 95% Confidence Intervals (10,000 Iterations)

| Metric | Empirical estimate (%) | Bootstrap mean (%) | Standard deviation (%) | 95% CI lower limit (%) | 95% CI upper limit (%) |
|---|---|---|---|---|---|
| Observation-based reliability (Robs*Robs*) | 35.63 | 35.63 | 0.451 | 34.75 | 36.53 |
| Duration-based reliability (Rtime*Rtime*) | 36.63 | 36.63 | 0.635 | 35.38 | 37.88 |

As detailed in Table 10, the bootstrap mean for observation-based reliability converged exactly at 35.63%, with an empirical standard deviation of 0.451 percentage points and a tight 95% confidence interval of 34.75%–36.53%. For duration-based reliability, the bootstrap mean was 36.63%, with a standard deviation of 0.635 percentage points and a 95% confidence interval of 35.38%–37.88%.

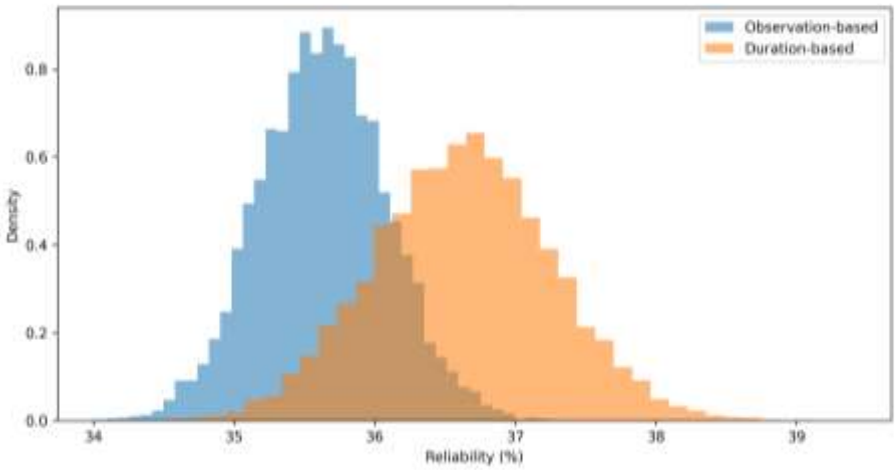


Figure 6. Bootstrap Resampling Distributions and 95% Confidence Intervals for Observation-Based and Duration-Based Reliability (10,000 Iterations)

The narrow confidence boundaries displayed in Figure 6 indicate that the sample size of 11,166 sailing records provides high inferential stability, confirming that the empirical service-speed compliance rate hovers reliably around 35.6%–36.6% across the observed crossing operations.

## 4.2 Discussion

Discussion The empirical results demonstrate that compliance with the prescribed 7–9 knot service-speed envelope was relatively limited across the observed Ro-Ro ferry operations. The observation-based reliability was 35.63%, the duration-based reliability was 36.63%, and the Weibull CDF yielded a parametric compliance probability of 35.88%. The close concordance among these three estimates—specifically the narrow 1.00 percentage-point differential between observation- and duration-based reliability—confirms that the overarching finding is highly consistent across distinct analytical formulations. However, these figures must be interpreted strictly as service-speed compliance rather than indicators of mechanical reliability, navigational accident risk, or total ferry service failure. The observed non-compliance was overwhelmingly characterized by sub-threshold sailing speeds. Both the fleet mean SOG (6.74 knots) and median SOG (6.70 knots) fell below the 7-knot lower compliance threshold. This operational pattern is further substantiated by the fitted Weibull distribution, where $$F(7) = 0.5438$$, demonstrating that 54.38% of the active sailing speed distribution was concentrated at or below 7 knots, compared to only 9.74% exceeding the 9-knot ceiling. Thus, the dominant mode of operational non-compliance was under-speed sailing rather than excessive speeding.

Potential contributing factors include hull fouling, engine power derating, heavy vehicle payloads, traffic congestion within the narrow crossing corridor, cautionary maneuvering in restricted waters, or counter-current resistance. From an operational perspective, persistent under-speed navigation inevitably prolongs crossing durations, triggers schedule-delay ripple effects across consecutive round trips, and exacerbates dockside vehicle congestion during peak transit hours. Nevertheless, specific causal attribution cannot be conclusively established from an AIS-only kinematic analysis. The duration-based formulation complements the discrete observation-based indicator by explicitly compensating for non-uniform AIS transmission intervals. The marginal difference between the two metrics indicates that the primary compliance conclusions were not unduly distorted by observation sampling density. Furthermore, the 1,285 identified reliable-speed segments exhibited a mean duration of 15.16 minutes and a median of 13.10 minutes, against a maximum continuous duration of 40.93 minutes. This reveals that compliant operations occurred predominantly as fragmented operational bursts rather than sustained, continuous cruising legs. Consequently, service-speed reliability in short-sea ferry services must be evaluated not merely by whether vessels attain prescribed speeds, but also by their capacity to sustain compliant speeds over meaningful operational durations. Substantial vessel-level performance heterogeneity was also uncovered within the fleet. KMP BN and KMP SP demonstrated robust compliance, recording duration-based reliabilities of 61.52% and 53.68% with average speeds of 7.21 and 7.76 knots, respectively. Conversely, KMP SD and KMP MP2 operated almost entirely outside the service-speed standard, achieving duration reliabilities of only 7.40% and 5.47% with mean speeds of 5.59 and 5.39 knots.

These pronounced disparities indicate a structural "two-tier" operational polarization within the fleet, wherein chronically underperforming vessels act as systemic bottlenecks along the corridor. Relying solely on fleet-wide aggregate metrics would entirely mask this individual deficiency. In practical terms, this finding demonstrates that maritime regulators and fleet managers should avoid uniform fleet policies and instead adopt targeted operational interventions, differentiated maintenance schedules, and vessel-specific timetable allocations. Nonetheless, standalone AIS kinematic trajectories cannot determine whether these operational discrepancies stem from mechanical deterioration, divergent propulsion capacities, differing loading regimes, or distinct operational assignments. The probability distribution analysis further reinforces the statistical coherence of the empirical reliability estimates. Among the four candidate models, the Weibull distribution achieved superior goodness-of-fit, yielding the lowest AIC (44,051.48) and BIC (44,073.44) and outperforming the second-best Normal distribution by an AIC margin of 58.80. The Weibull CDF-derived compliance probability of 35.88%, computed via $$P(7 \le \text{SOG} \le 9) = F(9) - F(7)$$, aligns remarkably with the empirical observation-based reliability of 35.63%. This confirms that parametric CDF modeling provides a valid continuous representation of service-speed compliance, although it remains a model-based approximation conditioned on distribution selection. The temporal analysis revealed a progressive decline in operational compliance across the first quarter of 2026. Observation-based reliability diminished from 38.54% in January to 35.42% in February and 34.09% in March, mirrored by a corresponding contraction in duration-based reliability from 39.88% to 34.13%.

The synchronized trajectory of both metrics indicates that this degradation was not an artifact of varying AIS message transmission densities. Notably, March recorded the highest volume of sailing observations (4,494 records) but the lowest compliance rate, reiterating that raw compliant observation counts must always be contextualized against total operating exposure. Because external environmental and operational variables—such as tidal stream variations, monsoonal sea states, passenger-cargo demand fluctuations, and dockside turnaround constraints—were not captured, this temporal decline serves as a descriptive operational pattern rather than definitive proof of systemic degradation. The non-parametric bootstrap resampling analysis verifies the high estimation stability of the empirical metrics. Resampling across 10,000 iterations produced narrow 95% confidence intervals of 34.75%–36.53% for observation-based reliability and 35.38%–37.88% for duration-based reliability. These constrained bounds confirm that the approximately 36% baseline compliance estimate is statistically robust against sampling variability. Crucially, however, statistical stability must not be conflated with operational adequacy. The bootstrap analysis proves the precision of the estimator within the sample space; it does not imply that a 36% compliance rate satisfies regulatory or public transport service expectations. Overall, the findings demonstrate that AIS-derived SOG provides a powerful, screening-level diagnostic indicator for maritime transport oversight. By combining observation compliance, duration weighting, directional failure analysis, vessel disaggregation, parametric modeling, and resampling uncertainty, the framework delivers actionable visibility into ferry corridor operations without requiring intrusive on-board data logging.

The aggregate finding that only approximately one-third of active sailing exposure complies with the mandated 7–9 knot envelope provides immediate diagnostic utility for transport authorities and ferry operators seeking early-stage performance auditing where detailed trip manifests are inaccessible. Furthermore, from a policy perspective, such low overall compliance suggests that transportation authorities should critically re-evaluate whether the 7–9 knot regulatory envelope aligns with prevailing hydrodynamic constraints, or whether intensified enforcement and dry-dock inspections are required for chronically non-compliant tonnage. Nonetheless, several methodological boundaries must be acknowledged. First, the observation-level architecture of this study relies strictly on kinematic filtering (3–15 knots) and does not reconstruct full berth-to-berth trip itineraries; thus, it does not explicitly isolate terminal maneuvering, fairway navigation, waiting at anchor, or port approach phases. Consequently, an individual observation outside the 7–9 knot envelope must not be interpreted as an operational failure in isolation. Second, the 7–9 knot service envelope represents a route-specific regulatory standard; therefore, the quantitative reliability levels reported here cannot be directly extrapolated to other maritime corridors without calibrating for local navigational constraints and licensing mandates. Future research should advance this framework by integrating AIS trajectories with automated voyage-segmentation algorithms, terminal event logging, metocean hindcasts (wind, waves, tides, and currents), vessel displacement data, and maintenance records, thereby expanding this screening-level indicator into a fully integrated, trip-level ferry service reliability model.

## 5. Conclusion and Recommendations

This study developed and demonstrated a simplified, AIS-based probabilistic framework for evaluating Ro-Ro ferry service reliability through service-speed compliance. Applying a baseline sailing filter of 3–15 knots and a route-specific regulatory service envelope of 7–9 knots retained 11,166 active sailing observations from 32,358 raw AIS messages across four commercial vessels. The empirical analysis yielded an observation-based reliability of 35.63% and a duration-based reliability of 36.63%, representing 324.76 compliant sailing hours out of 886.64 total valid operating hours. Continuous parametric modeling identified the Weibull distribution as the superior fit based on information criteria, yielding an interval compliance probability of 35.88% via its cumulative distribution function. The high degree of concordance among the observation-based, duration-based, and parametric CDF estimates demonstrates that service-speed compliance consistently hovers around 36% across analytical formulations. Furthermore, non-parametric bootstrap resampling yielded narrow 95% confidence intervals (34.75%–36.53% for observations and 35.38%–37.88% for duration), confirming the inferential stability of the estimates within the sample space. The primary contribution of this research lies in establishing an accessible, dual-metric probabilistic framework that bridges kinematic observation counts and temporal sailing exposure, reinforced by parametric distribution modeling and resampling-based uncertainty quantification. This provides maritime transportation authorities, port administrators, and vessel operators with a cost-effective, non-intrusive screening tool capable of converting standard AIS broadcasts into actionable service-performance diagnostics. Moreover, the disaggregated framework effectively exposes operational heterogeneity across individual vessels and temporal shifts across operating months—nuances that are routinely obscured by traditional aggregate reporting. The analytical pipeline is readily transferable to other short-sea ferry corridors, provided that route-specific speed envelopes and preprocessing parameters are properly established.

Notwithstanding these contributions, several limitations define the boundaries of the present study. The empirical results remain contextual to the observed corridor and observation timeframe. Operating strictly at the kinematic observation level, the framework does not incorporate ground-truth voyage schedules, cargo displacement manifests, terminal approach milestones, or environmental conditions such as wind, tidal currents, and sea states. Consequently, the methodology detects speed-compliance patterns rather than establishing causal attribution for performance deficits. Future research should advance this screening-level model into a comprehensive, trip-level service reliability architecture by integrating AIS trajectory segmentation, automated berth-to-berth trip reconstruction, terminal-event detection, and hydrodynamic covariates. Such multi-source integration will enable analysts to decouple normal navigational maneuvering and terminal queuing from structural service degradation, ultimately providing a holistic foundation for maritime transit planning and regulatory enforcement.

## References

Amuta, E. O., Wara, S. T., Agbetuyi, A. F., & Sawyerr, B. A. (2022). Weibull distribution-based analysis for reliability assessment of an isolated power micro-grid system. *Materials Today: Proceedings*, *65*, 2215–2220. https://doi.org/10.1016/j.matpr.2022.06.244

Arekar, K., Jain, R., & Kumar, S. (2021). Bayesian estimation of system reliability models using Monte-Carlo technique of simulation. *Journal of Statistical Theory and Applications*, *20*(1), 149–163. https://doi.org/10.2991/jsta.d.210201.001

Betz, W., Papaioannou, I., & Straub, D. (2022). Bayesian post-processing of Monte Carlo simulation in reliability analysis. *Reliability Engineering & System Safety*, *227*, Article 108731. https://doi.org/10.1016/j.ress.2022.108731

Capobianco, S., Millefiori, L. M., Forti, N., Braca, P., & Willett, P. (2021). Deep learning methods for vessel trajectory prediction based on recurrent neural networks. *IEEE Transactions on Aerospace and Electronic Systems*, *57*(6), 4329–4346. https://doi.org/10.1109/TAES.2021.3096873

Clavijo-Blanco, J. A., González-Cagigal, M. A., & Rosendo-Macías, J. A. (2024). Statistical characterization of reliability indices in medium voltage networks using a Monte Carlo-based method. *Electric Power Systems Research*, *234*, Article 110585. https://doi.org/10.1016/j.epsr.2024.110585

Deriba, A. Z., & Yang, D. Y. (2025). Performance-based risk assessment for large-scale transportation networks using the transitional Markov chain Monte Carlo method. *ASCE-ASME Journal of Risk and Uncertainty in Engineering Systems, Part A: Civil Engineering*, *11*(1), Article 04024090. https://doi.org/10.1061/AJRUA6.RUENG-1402

Gómez, Y. M., Gallardo, D. I., Marchant, C., Sánchez, L., & Bourguignon, M. (2024). An in-depth review of the Weibull model with a focus on various parameterizations. *Mathematics*, *12*(1), Article 56. https://doi.org/10.3390/math12010056

Labeau, P. E., & Zio, E. (2002). Procedures of Monte Carlo transport simulation for applications in system engineering. *Reliability Engineering & System Safety*, *77*(3), 217–228. https://doi.org/10.1016/S0951-8320(02)00055-8

Li, H., Jiao, H., & Yang, Z. (2023a). AIS data-driven ship trajectory prediction modelling and analysis based on machine learning and deep learning methods. *Transportation Research Part E: Logistics and Transportation Review*, *175*, Article 103152. https://doi.org/10.1016/j.tre.2023.103152

Li, H., Jiao, H., & Yang, Z. (2023b). Ship trajectory prediction based on machine learning and deep learning: A systematic review and methods analysis. *Engineering Applications of Artificial Intelligence*, *126*, Article 107062. https://doi.org/10.1016/j.engappai.2023.107062

Li, Z., Fu, H., & Guo, J. (2025). Reliability assessment of a series system with Weibull-distributed components based on zero-failure data. *Applied Sciences*, *15*(5), Article 2869. https://doi.org/10.3390/app15052869

Liang, M., Su, J., Liu, R. W., & Lam, J. S. L. (2024). AISClean: AIS data-driven vessel trajectory reconstruction under uncertain conditions. *Ocean Engineering*, *306*, Article 117987. https://doi.org/10.1016/j.oceaneng.2024.117987

Martinčič, T., Štepec, D., Costa, J. P., Čagran, K., & Chaldeakis, A. (2020). Vessel and port efficiency metrics through validated AIS data. In *Global Oceans 2020: Singapore–U.S. Gulf Coast* (pp. 1–6). IEEE. https://doi.org/10.1109/IEEECONF38699.2020.9389112

Nguyen, D., Simonin, M., Hajduch, G., Vadaine, R., Tedeschi, C., & Fablet, R. (2020). Detection of abnormal vessel behaviours from AIS data using GeoTrackNet: From the laboratory to the ocean. In *2020 21st IEEE International Conference on Mobile Data Management (MDM)* (pp. 264–268). IEEE. https://doi.org/10.1109/MDM48529.2020.00061

Nie, Y., Li, J., Liu, G., & Zhou, P. (2023). Cascading failure-based reliability assessment for post-seismic performance of highway bridge network. *Reliability Engineering & System Safety*, *238*, Article 109457. https://doi.org/10.1016/j.ress.2023.109457

Oszczypała, M., Ziółkowski, J., & Małachowski, J. (2023). Modelling the operation process of light utility vehicles in transport systems using Monte Carlo simulation and semi-Markov approach. *Energies*, *16*(5), Article 2210. https://doi.org/10.3390/en16052210

Pokorádi, L. (2024). Monte-Carlo simulation of reliability of system with complex interconnections. *Vehicles*, *6*(4), 1801–1811. https://doi.org/10.3390/vehicles6040087

Singh, S. K., & Heymann, F. (2020). Machine learning-assisted anomaly detection in maritime navigation using AIS data. In *2020 IEEE/ION Position, Location and Navigation Symposium (PLANS)* (pp. 832–838). IEEE. https://doi.org/10.1109/PLANS46316.2020.9109806

Vukša, S., Vidan, P., Bukljaš, M., & Pavić, S. (2022). Research on ship collision probability model based on Monte Carlo simulation and Bi-LSTM. *Journal of Marine Science and Engineering*, *10*(8), Article 1124. https://doi.org/10.3390/jmse10081124

Wang, N., & Yuen, K. F. (2022). Resilience assessment of waterway transportation systems: Combining system performance and recovery cost. *Reliability Engineering & System Safety*, *226*, Article 108673. https://doi.org/10.1016/j.ress.2022.108673

Wolsing, K., Roepert, L., Bauer, J., & Wehrle, K. (2022). Anomaly detection in maritime AIS tracks: A review of recent approaches. *Journal of Marine Science and Engineering*, *10*(1), Article 112. https://doi.org/10.3390/jmse10010112

Xin, X., Liu, K., Yang, Z., Zhang, J., & Wu, X. (2021). A probabilistic risk approach for the collision detection of multi-ships under spatiotemporal movement uncertainty. *Reliability Engineering & System Safety*, *215*, Article 107772. https://doi.org/10.1016/j.ress.2021.107772

Yan, Z., Xiao, Y., Cheng, L., He, R., Ruan, X., Zhou, X., Li, M., & Bin, R. (2020). Exploring AIS data for intelligent maritime routes extraction. *Applied Ocean Research*, *101*, Article 102271. https://doi.org/10.1016/j.apor.2020.102271

Yang, C.-H., Wu, C.-H., Shao, J.-C., Wang, Y.-C., & Hsieh, C.-M. (2022). AIS-based intelligent vessel trajectory prediction using Bi-LSTM. *IEEE Access*, *10*, 24302–24315. https://doi.org/10.1109/ACCESS.2022.3154812

Yang, D., Wu, L., Wang, S., Jia, H., & Li, K. X. (2019). How big data enriches maritime research: A critical review of automatic identification system (AIS) data applications. *Transport Reviews*, *39*(6), 755–773. https://doi.org/10.1080/01441647.2019.1649315

Yang, Y., Liu, Y., Li, G., Zhang, Z., & Liu, Y. (2024). Harnessing the power of machine learning for AIS data-driven maritime research: A comprehensive review. *Transportation Research Part E: Logistics and Transportation Review*, *183*, Article 103426. https://doi.org/10.1016/j.tre.2024.103426

Zang, Z., Xu, X., Qu, K., Chen, R., & Chen, A. (2022). Travel time reliability in transportation networks: A review of methodological developments. *Transportation Research Part C: Emerging Technologies*, *143*, Article 103866. https://doi.org/10.1016/j.trc.2022.103866

Zohoori, S., Jafari Kang, M., Hamidi, M., & Maihami, R. (2023). An AIS-based approach for measuring waterway resiliency: A case study of Houston ship channel. *Maritime Policy & Management*, *50*(6), 797–817. https://doi.org/10.1080/03088839.2022.2047813